

6. CALCAREOUS-NANNOFOSSIL BIOSTRATIGRAPHY, NAURU BASIN, DEEP SEA DRILLING PROJECT SITE 462, AND UPPER CRETACEOUS NANNOFACIES¹

Hans R. Thierstein, Scripps Institution of Oceanography, University of California, San Diego, La Jolla, California

and

Helène Manivit, C.N.R.S. and Laboratoire de Palynologie, BRGM, B.P. 6009, 45018 Orleans Cedex, France

ABSTRACT

The deep-sea sediments recovered at Deep Sea Drilling Project Site 462 are of middle Cretaceous through Pleistocene age. The biostratigraphic age assignments based on calcareous nannofossils as given in the Site Summary (this volume) are documented here in detail, and an attempt to recognize the depth-provenance of Upper Cretaceous nannofossil carbonate in the nannofacies is explained and illustrated.

BIOSTRATIGRAPHY

Holes 462 and 462A were drilled in the Nauru Basin (western central Pacific), in 5189 and 5186 meters of water. They are at the foot of the northeastern slope of the Ontong-Java Plateau, at 07°14'N and 165°02'E, slightly off the up-slope axis of a northeast-trending deep-sea channel (Fig. 1). This topographic setting is reflected in the lithologies of the sediments and in the composition of most microfossil assemblages recovered. The sediments from large parts of the section are fine-grained, distal turbidites. Particularly in the Neogene sequence, the calcareous nannofossils, as observed in smear slides under the light microscope, are packed in radiolarian-test fragments, which are dominantly in the 20- to 50- μ m size range. Comparatively few, isolated coccoliths were observable in these slides; in many cases the radiolarian tests had to be crushed and the coccoliths dispersed on the slide to provide a sufficient number of isolated and identifiable nannofossil specimens. Apparent lateral transport of sediment particles also resulted in mixed fossil assemblages, in which the reworked portion of the nannoflora often exceeded the younger, indigenous portion. Some of the apparent age discrepancies among the various microfossil groups (Figs. 2-4; Site Summary, this volume) may be related to these differential-transport mechanisms. Other biostratigraphic inconsistencies, as in the sediments in Cores 5 to 8, may be related to hole collapse, favored by the sandy nature of the sediments in the uppermost part of the hole.

The abundance, preservation, and stratigraphic distribution of identified calcareous nannofossils are listed in Figures 5 to 8 (Figs. 5 and 7 are in back pocket, this volume).

The full generic and specific names of all taxa considered in this report, and references to authors, are given in Table 1. The estimated relative abundances of each taxon as shown in Figures 5 to 8 are on a logarithmic

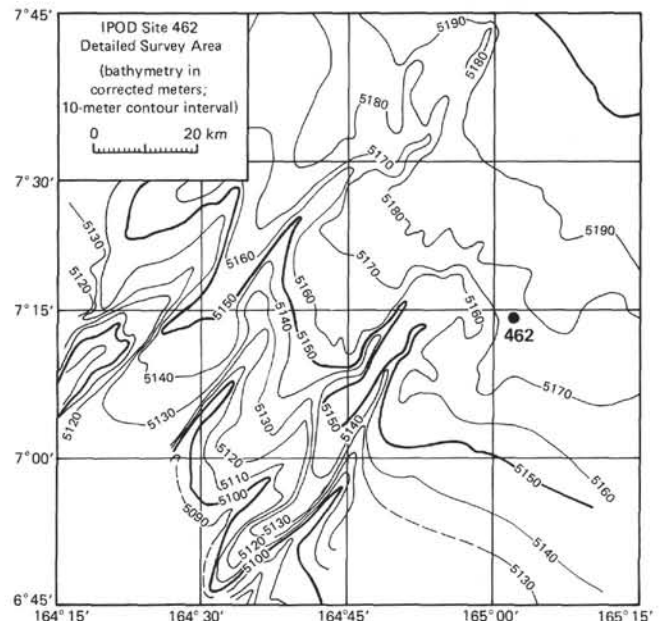


Figure 1. Geographic and bathymetric location of Site 462.

mic scale. Lower-case letters indicate that the taxon is considered reworked. Abundances and preservational data given in the left-hand column next to the sub-bottom depths, refer to the whole assemblage. Preservation is described as etching or overgrowth, both on a scale of 0 to 3, following the scheme developed by Roth and Thierstein (1972). The estimated proportion of reworked nannofossils in the examined assemblages is also listed in the left-hand column. The Cenozoic range charts for Holes 462 and 462A (Figs. 5 [back pocket] and 6) include the encountered taxa that were considered stratigraphically useful. The zonal scheme indicated is Martini's (1971) numbered standard zonation; stratigraphic criteria from Bukry (1973, 1975), however, have also been used with the correlation between the two zonal schemes as given in Bukry (1978). The Mesozoic range charts (Figs. 7 [back pocket] and 8) show all recognizable nannofossil taxa. The Campanian

¹ Initial Reports of the Deep Sea Drilling Project, Volume 61.

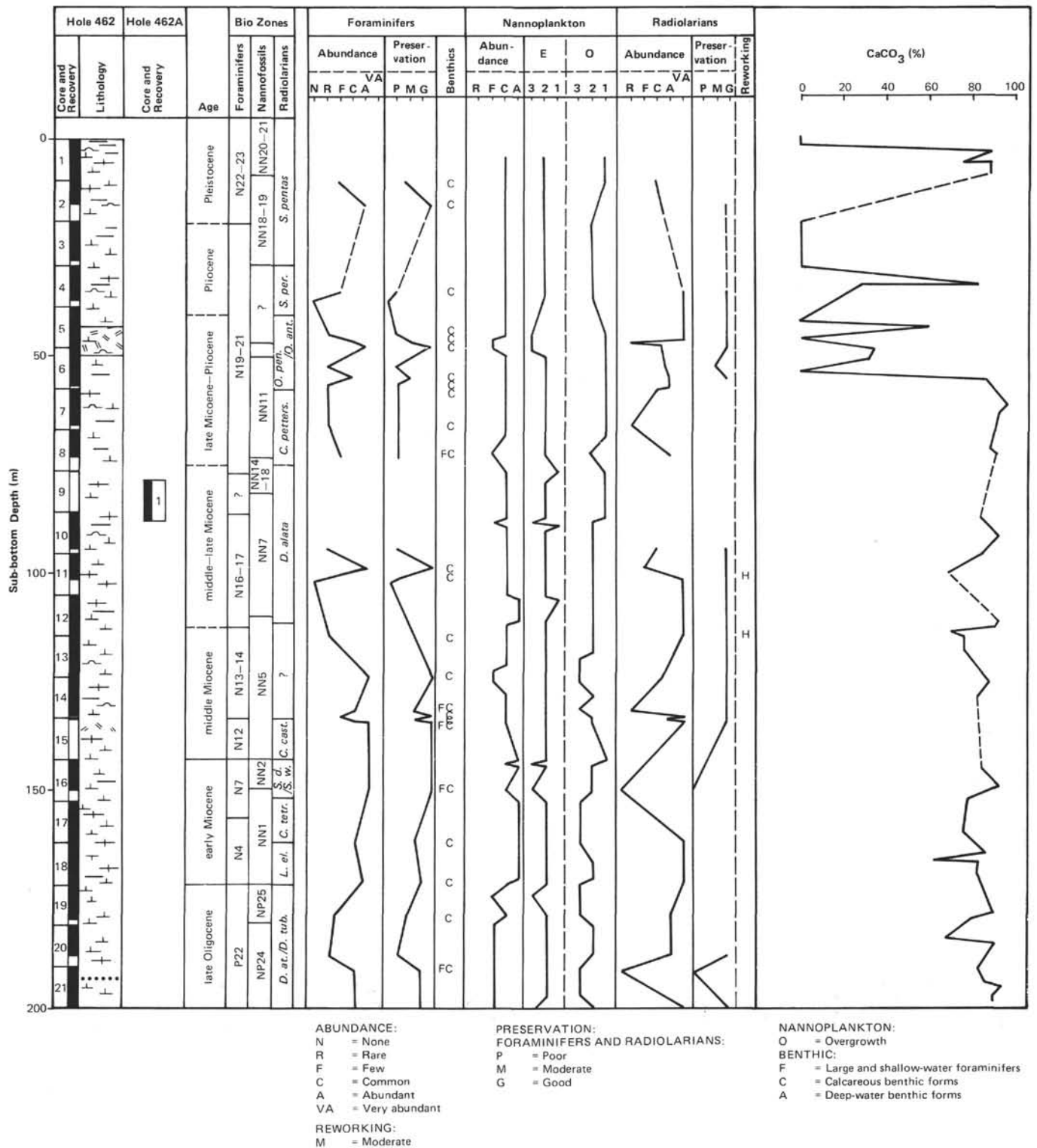


Figure 2. Neogene stratigraphy of Site 462 (see also Site Summary, this volume).

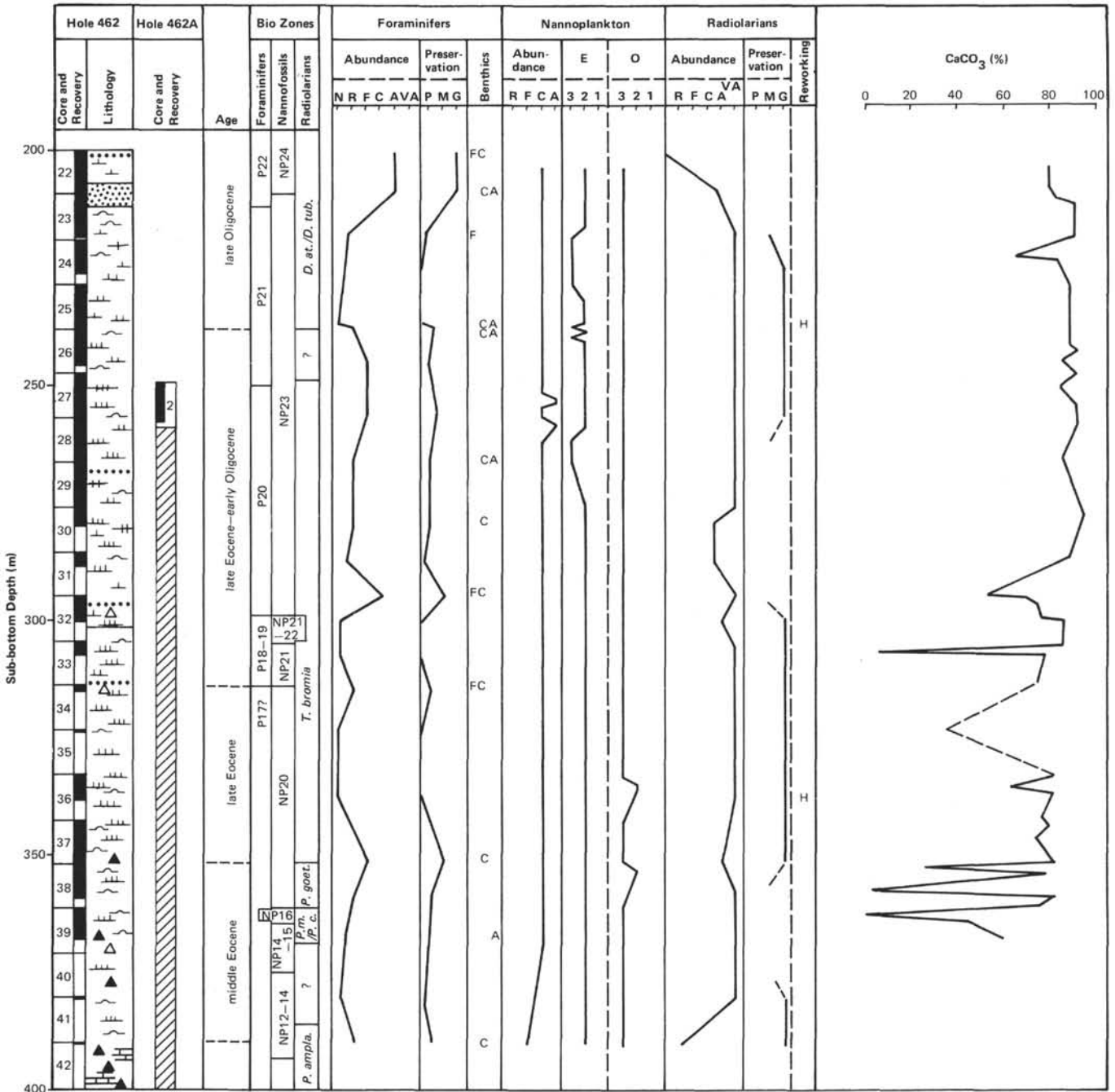


Figure 3. Paleogene stratigraphy of Site 462 (see also Site Summary, this volume). Symbols as in Figure 2.

and Maestrichtian zonation is that proposed by Verbeek (1977). Pre-Campanian assemblages cannot be assigned readily to a particular zone. Stratigraphic correlations are discussed individually below.

Core 1 (0-9 m)

Pleistocene, based on the appearance of *G. oceanica* and the abundance and decrease of *P. lacunosa*, and on the planktonic foraminifers.

Cores 2 through 5 (9-48 m)

Late Pliocene to Pleistocene, based on the presence of *G. caribbeanica*, *C. cristatus*, *P. lacunosa*, and *D. asymmetricus*, and the abundance of *D. brouweri*, *D. pentaradiatus*, and *D. surculus*. This age assignment is in agreement with the planktonic foraminifers. The presence of Pliocene *D. asymmetricus* in Core 4, and of *C. cristatus* in Core 5, indicates that the late Miocene radiolarians in these cores must be reworked.

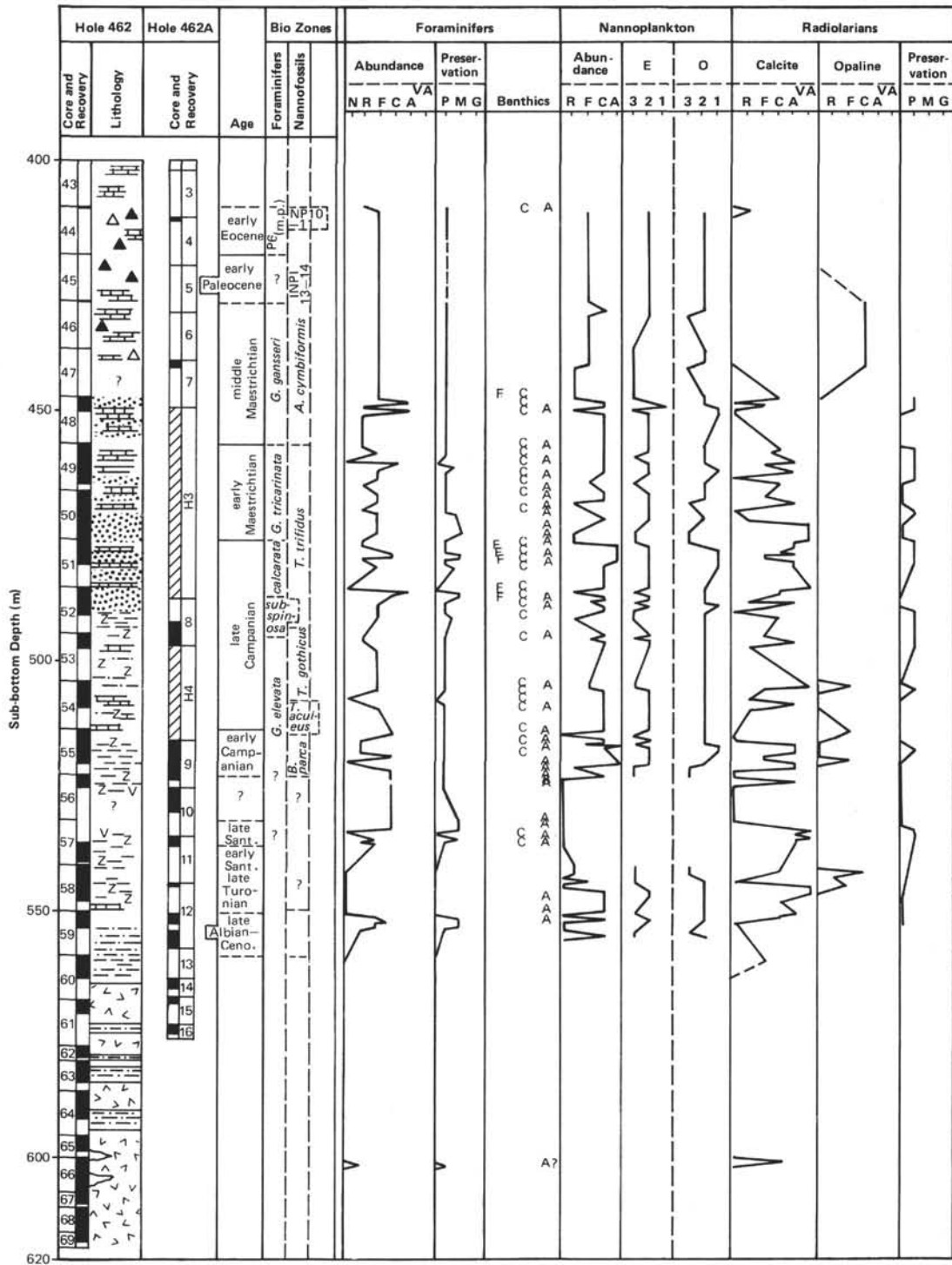


Figure 4. Mesozoic stratigraphy of Site 462 (see also Site Summary, this volume). Symbols as in Figure 2.

Cores 6 through 8 (49–76 m)

Stratigraphic interpretation of this sequence is ambiguous. All samples examined in this interval (see Fig. 5), with the exception of 8,CC, contain late Miocene nannofossil assemblages. This age assignment is corroborated by radiolarians. The nannofossil assemblage from 8,CC contains latest Pliocene or younger species, such as *G. caribbeanica*, *C. cristatus*, and *P. lacunosa*,

which however would be considerably younger than the early Pliocene foraminifers encountered in Cores 7 and 8 (Premoli Silva and Violanti, this volume). The possibility of down-hole contamination cannot be ruled out.

Core 1A, Cores 10 through 15 (79–143 m)

Middle Miocene, based on the presence of *D. kugleri* in Cores 1A, 10, 11, and the top of 12, and of *S. heteromorphus* and *D. exilis* in Cores 12 through 15. This age

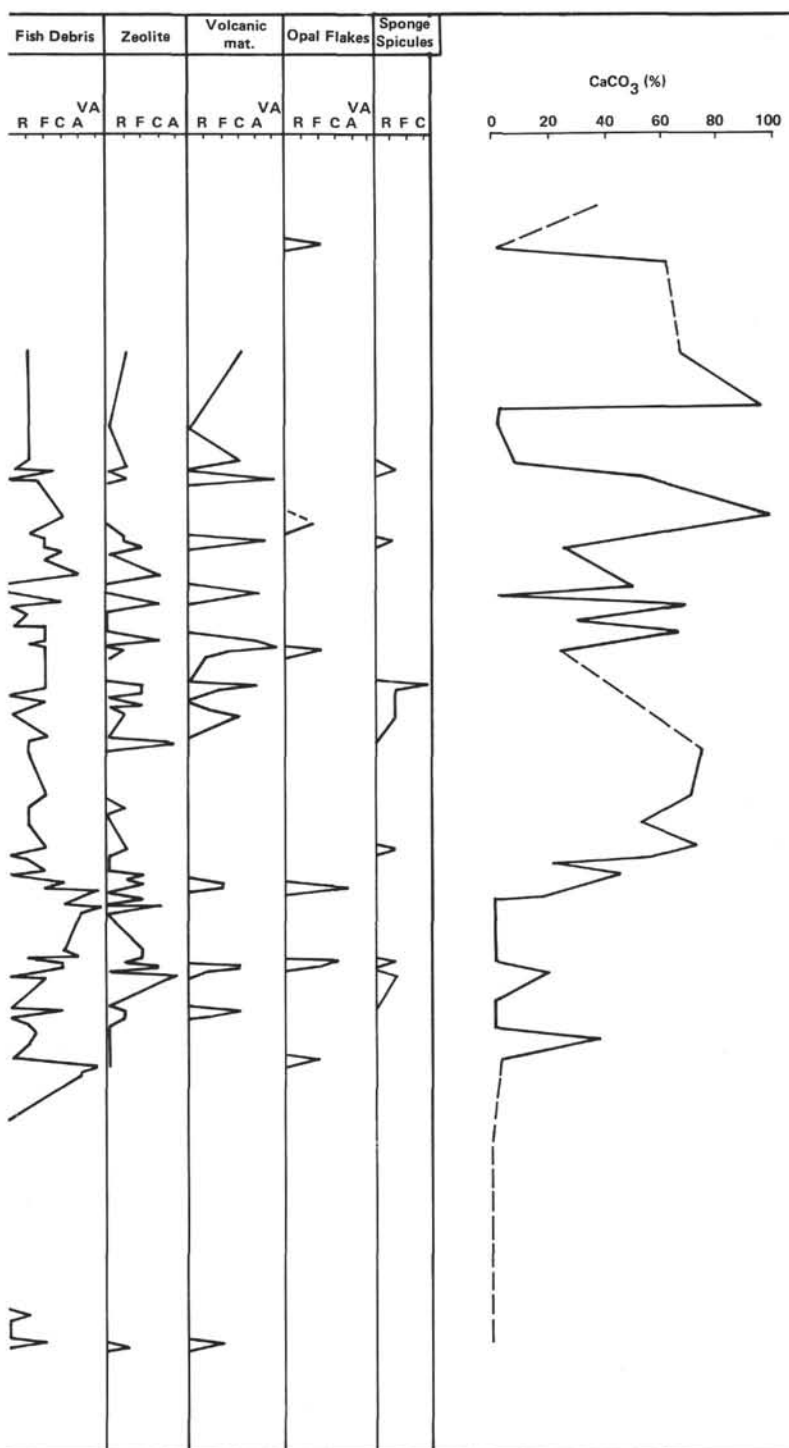


Figure 4. (Continued).

is confirmed by radiolarians. Planktonic foraminifers are interpreted as late Miocene in age. No late middle Miocene or late Miocene marker nannofossils could be identified in any of seven assemblages examined within this interval; their absence might, however, be due to moderate to poor preservation.

Cores 16 through 18 (150–171 m)

Early Miocene, based on the presence of *D. druggii* in Core 16, Section 1, and of *T. carinatus* in Core 16 through Core 19, Section 2. Radiolarians confirm this age. Planktonic-foraminifer assemblages are considered

Age	Nannofossil Zone	Sample (interval in cm)	Sub-bottom Depth (m)	Abundance	Preservation	Etching	Overgrowth	Reworking	<i>Sphenolithus abies</i>	<i>Cyclargolithus abisectus</i>	<i>Ceratolithus acutus</i>	<i>Discoaster asymmetricus</i>	<i>Discoaster barbadensis</i>	<i>Discoaster berggrenii</i>	<i>Zygrhabdithus bijugatus</i>	<i>Dictyococcites bisectus</i>	<i>Discoaster bollii</i>	<i>Discoaster brouweri</i>	<i>Discoaster calcaris</i>	<i>Catinaster calyculus</i>	<i>Gephyrocapsa caribbeanica</i>	<i>Triquetrorhabdulus carinatus</i>	<i>Helicosphaera carteri</i>	<i>Discoaster challengerii</i>	<i>Sphenolithus ciperoensis</i>	<i>Catinaster coelitus</i>	<i>Helicosphaera compacta</i>	<i>Ceratolithus cristatus</i>	<i>Chiasmolithus danicus</i>	<i>Discoaster deflandrei</i>	<i>Discoaster diastypus</i>	<i>Sphenolithus distentus</i>	<i>Crenolithus doronicoides</i>	<i>Discoaster druggii</i>	<i>Discoaster exilis</i>	<i>Cyclargolithus floridanus</i>				
late Miocene	NN7	1-1, 53-54	79.0	C	M	2	1	r	F																															
	NN7	1-6, 105-106	87.0	C	M	2	1	r	R																															
?	NN4-NN5	2-1, 90-91	250.4	A	P	2	3	f																																
early Oligocene	NP23	2,CC	259.0	A	P	2	3	r							A																									
	NP23	H1-7, 77-79		A	P	2	3	r						r	A													R												
Eocene	late	NP20	H1,CC		A	P	2	3	r				F		F																									
	middle	NP15	H2-1, 0-2		R	P	3	3																																
	early	NP10-NP12	5,CC	430.0	C	M	2	2	r																															

Figure 6. Stratigraphic distribution of Cenozoic calcareous nannofossils in Hole 462A. Symbols as in Figure 5 (back pocket, this volume).

to be somewhat younger, although still early Miocene, by Premoli Silva and Violanti (this volume).

Cores 19 through 32, Section 2, Core 2A (174-297 m)

Late Oligocene, based on the occurrence of *S. ciperoensis* in Cores 19 through 22, and *S. distentus* in Core 19 to Core 32, Section 2. The early/late Oligocene boundary is placed in Core 32, based on planktonic-foraminifer evidence. The radiolarians are of late Eocene age below Core 27, Section 2, and are considered reworked, an interpretation that is supported by abundant late Eocene nannofossils and very rare Oligocene marker species encountered in this interval.

Cores 32 (bottom) and 33 (304-314 m)

Early Oligocene, based on the absence of *D. saipanensis* in Core 33. Planktonic foraminifers confirm this age assignment; whereas radiolarians indicate a late Eocene age and may be reworked.

Cores 34 to 38 (314-361.5 m)

Late Eocene, based on the co-occurrence *S. moriformis*, *S. pseudoradians*, *H. reticulata*, and *D. saipanensis* in Cores 34 through 38. This age assignment correlates well with the planktonic foraminifers and radiolarian ages.

Core 39 (361.5-371 m)

Middle Eocene, based on the co-occurrence of *S. furcatolithoides*, *C. grandis*, *D. kuepperi*, *C. solitus*, and *R. umbilica*.

Cores 40 through 44, and Core 5A (390-410 m)

Early Eocene, based on the occurrence of *D. barbadensis*, *D. diastypus*, *C. formosus*, and *D. multiradiatus* in some or all samples from Cores 40 through 44. This age is in agreement with that inferred from planktonic foraminifers. The lowermost Cenozoic radiolarian assemblage encountered at this site is from Core 41 and is considered of middle Eocene age.

Core 45 (428 m)

Early Paleocene, based on the presence of *C. danicus*, *Z. sigmoides*, and *C. tenuis*.

Core 46 through Core 48, Section 2, Core 7A (437-449 m)

Middle Maestrichtian, based on the absence of *T. gothicus*, *T. trifidus*, and *L. quadratus*. This age assignment is confirmed by the planktonic foraminifers.

Cores 48 (bottom) through Core 52, Core 8A (top) 456-494 m)

Late Campanian to early Maestrichtian, based on the presence of *T. trifidus*. This age is confirmed by the planktonic foraminifers.

Cores 53 through 54, Core 8A (below Section 1) (489-512 m)

Late Campanian, based on presence of *C. aculeus* and *T. gothicus*. This age assignment agrees with the evidence from planktonic foraminifers.

Core 55 and Core 9A (514-522.5 m)

Early Campanian, based on the presence of *B. parca*. Planktonic foraminifers confirm this age assignment.

Core 56 through Core 58, Core 11A, Core 12A (upper part) (522.5-549 m)

Turonian to Santonian, based on the presence of *M. decoratus*, *M. staurophora*, and *L. floralis* in this interval, as well as on the age of the nannofossil assemblages above and below. There is no contrary evidence from the few poorly preserved planktonic-foraminifer assemblages encountered in Core 57.

Core 59, Section 1, Core 12A (lower part), and Core 13A (top) (549-553 m)

Late Albian to Cenomanian, based on the co-occurrence of *C. chiastia*, *C. signum*, *E. turriseiffelii*, and

Age	Nannofossil Zone	Sample (interval in cm)	Sub-bottom Depth (m)	Abundance	Preservation	Etching	Overgrowth	Reworking	<i>Tetralithus aculeus</i>	<i>Lithraphidites alatus</i>	<i>Parahabdolithus angustus</i>	<i>Reinhardtites anthophorus</i>	<i>Parahabdolithus asper</i>	<i>Watznaueria barnesae</i>	<i>Lithraphidites carniolensis</i>	<i>Lucianorhabdus cayeuxii</i>	<i>Crucellipsis chiastra</i>	<i>Markalius circumradiatus</i>	<i>Vagalapilla compacta</i>	<i>Creterhabdus conicus</i>	<i>Biscutum constans</i>	<i>Creterhabdus crenulatus</i>	<i>Prediscosphaera cretacea</i>	
Maestrichtian	<i>A. cymbiformis</i>	7-1, 96-100	440.5	C	P	3	2	r						A	F									
		3H-3, 75-79		F	P	3	2							A	R								F	
Campanian	<i>T. trifidus</i>	3H,CC		C	P	3	2		R				R	A									R	
		8-1, 57-60	487.6	C	P	3	2		F					A									R	
		8-2, 128-134	489.8	C	P	3	2		C					A	F									R
	<i>T. gothicus</i>	8,CC	496.5	R	P	3	2		R					R	R									
		4H-3, 112-115			F	P	3	2						R										
	<i>T. aculeus</i>	4H,CC		R	P	3	2		R					R										
early	<i>B. parca</i>	9-1, 35-41	515.9	F	P	3	2							A	F								F	
		9-2, 70-76	517.2	C	M	2	1							A	R								F	
		9-4, 6-10	520.6	C	P	3	3								A	R							F	
		9-5, 80-84	522.3	C	P	2	3								A	C								R
Cenomanian?		10-1, 47-52	525.5	B					(7 barren samples)															
		11-2, 6-9	536.1	B					(7 barren samples)															
		11,CC	544.0	R	P	3	3							R									R	
		12-1, 5-6	544.1	B																				
		12-1, 62-67	544.6	B																				
		12-2, 2	545.5	R	P	3	3							R										
		12-2, 4-6	545.6	F	P	3	2		?					A				R					R	
		12,CC	553.4	R	P	3	3							R										
		13-1, 1-5	553.5	C	P	3	2		?					A		F								
		13-1, 7	553.6	F	P	3	2							A	F	R								R
l. Aptian to e. Albian?		13-1, 47	554.0	B					(21 barren samples)															
		32,CC	658.0	B					(21 barren samples)															
		40-1, 92	702.0	R	P	3	3						R	A			R							

Figure 8. Stratigraphic distribution of Mesozoic calcareous nannofossils in Hole 462A. Symbols as in Figure 5 (back pocket, this volume).

tive evidence for transport found in the lithology and the benthic deep-water foraminifers (Sliter, this volume). We have studied the nannofacies of the lowermost part of the Upper Cretaceous carbonate sequence which was recovered below the obviously transported volcanoclastic upper Campanian to lower Maestrichtian interval. The analyzed sequence consists of partially burrowed, interlayered claystones, marlstones, and limestones in Cores 54 and 55, from a sub-bottom depth of 509 to 522.5 meters. Within that interval, we have examined the nannofacies of 20 samples. Eleven of these samples, covering the characteristic lithologies, are dis-

cussed in detail below (see Table 2). Listed in Table 2 are the abundance of calcareous nannofossils, the inferred provenance (autochthonous or allochthonous) of benthic foraminifers (after Sliter, this volume), the per cent bulk calcium carbonate, and respective illustrations of the nannofacies.

We attempted to recognize differences in the nannofacies between intervals with apparently transported foraminifer assemblages and intervals with no evidence for transport in either the coarse fraction or the lithology. Features for transport might include changes in preservation of nannofossils, their average sizes, lami-

	Provenance of Benthic Foraminifers (from Sliter, this volume)													
	Indigenous Only	Some Transported	Most Transported											
Arkhangelskiella cymbiformis	R													
Microrhabdulus decoratus														
Zygodiscus diplogrammus		C												
Criboosphaerella ehrenbergii		C												
Parhabdololithus embergerii														
Lithastrinus floralis														
Tetralithus gothicus														
Lithraphidites helicoideus														
Assipetra infractetacea														
Rucinolithus irregularis														
Stephanolithion laffitei														
Chiastozygus litterarius														
Rucinolithus magnus														
Cyclagelosphaera magerelii														
Watznaeria oblonga	R													
Vagalapilla octoradiata	R													
Tranolithus orionatus														
Broinsonia parca														
Manivitella pemmatoidea														
Parhabdololithus regularis														
Discorhabdus rotatorius														
Corollithion signum														
Prediscosphaera spinosa														
Zygodiscus spiralis														
Parhabdololithus splendens														
Micula staurophora														
Tegumentum stradneri	F													
Vagalapilla stradneri														
Cretarhabdus surirellus	C													
Tetralithus trifidus	C													
Eiffellithus turrisseiffelii	C													
Braarudosphaera sp. 1														
Cylindralithus sp.	F													
Indigenous Only														
Some Transported														
Most Transported														

Figure 8. (Continued).

nations and preferred orientations, changes in the frequency of individual taxa and of coccospheres, degree of lithification, and possibly others.

The nannofacies was studied by Manivit with a scanning electron microscope (SEM), on broken surfaces of bulk samples. Methodology and terminology have previously been described by Noël (1968) and Noël and Melguen (1978). Differentiation of clay and carbonate particles was done with the aid of an ORTEC energy-dispersive X-ray system. The following discussion of the individual studied samples proceeds from bottom to top and refers to the illustrations in Plates 1 to 6.

Sample 462-55, CC (Plate 1, Figs. 4-6)

The dark-gray, silty claystone has a carbonate content of 16% and is at the base of the latest Cretaceous carbonate interval. None of the eight samples from the underlying 12 meters of zeolitic claystones contained any carbonate microfossils or measurable carbonate contents. Only two poorly preserved planktonic foraminifers (*Heterohelix* sp. and *Hedbergella* sp.) were recovered from this sample in the 63- to 50- μ m fraction. Rare and poorly preserved agglutinated benthic foraminifers are considered indigenous (Sliter, this volume).

Table 1. Calcareous-nannofossil taxa considered in this report.

Cenozoic
<i>Sphenolithus abies</i> Deflandre, 1954.
<i>Cyclicargolithus abisectus</i> (Müller, 1970) Bukry, 1973
<i>Ceratolithus acutus</i> Gartner and Bukry, 1974
<i>Discoaster asymmetricus</i> Gartner, 1969
<i>Discoaster barbadiensis</i> Tan 1927
<i>Discoaster berggrenii</i> Bukry, 1971
<i>Zygrhabdolithus bijugatus</i> (Deflandre, 1954) Deflandre, 1959
<i>Dictyococcites bisectus</i> (Hay, Mohler and Wade, 1966) Bukry and Percival, 1971
<i>Discoaster bollii</i> Martini and Bramlette, 1963
<i>Discoaster brouweri</i> Tan 1927
<i>Discoaster calcaris</i> Gartner, 1967
<i>Catinaster calyculus</i> Martini and Bramlette, 1963
<i>Gephyrocapsa caribbeanica</i> Boudreaux and Hay, 1967
<i>Triquetrorhabdulus carinatus</i> Martini, 1965
<i>Helicosphaera carteri</i> (Wallich, 1877) Kamptner, 1954
<i>Discoaster challengerii</i> Bramlette and Riedel, 1954
<i>Sphenolithus cipoensis</i> Bramlette and Wilcoxon, 1967
<i>Catinaster coalitus</i> Martini and Bramlette, 1963
<i>Helicosphaera compacta</i> Bramlette and Wilcoxon, 1967
<i>Ceratolithus cristatus</i> Kamptner, 1950
<i>Chiasmolithus danicus</i> (Broezen, 1959) Hay and Mohler, 1967
<i>Discoaster deflandrei</i> Bramlette and Riedel, 1954
<i>Discoaster diastypus</i> Bramlette and Sullivan, 1961
<i>Sphenolithus distentus</i> (Martini, 1965) Bramlette and Wilcoxon, 1967
<i>Crenolithus daronicoides</i> (Black and Barnes, 1961) Roth, 1973
<i>Discoaster druggi</i> Bramlette and Wilcoxon, 1967
<i>Discoaster exilis</i> Martini and Bramlette, 1963
<i>Cyclicargolithus floridanus</i> (Roth and Hay, 1967) Bukry, 1971
<i>Coccolithus formosus</i> (Kamptner, 1963) Wise, 1973
<i>Sphenolithus furcatolithoides</i> Locker, 1967
<i>Chiasmolithus grandis</i> (Bramlette and Sullivan, 1954) Radomski, 1968
<i>Chiasmolithus gigas</i> (Bramlette and Sullivan, 1954) Radomski, 1968
<i>Discoaster hamatus</i> Martini and Bramlette, 1963
<i>Sphenolithus heteromorphus</i> Deflandre, 1953
<i>Triquetrorhabdulus inversus</i> Bukry and Bramlette, 1969
<i>Fasciculithus involutus</i> Bramlette and Sullivan, 1961
<i>Heliolithus kleinpellii</i> Sullivan, 1964
<i>Discoasteroides kuepperi</i> (Stradner, 1959) Bramlette and Sullivan, 1961
<i>Discoaster kugleri</i> Martini and Bramlette, 1963
<i>Pseudoemiliania lacunosa</i> (Kamptner, 1963) Gartner, 1969
<i>Calcidiscus leptoporus</i> (Murray and Blackman, 1898) Loeblich and Tappan, 1978
<i>Discoaster lodoensis</i> Bramlette and Riedel, 1954
<i>Sphenolithus moriformis</i> (Bronnimann and Stradner, 1960) Bramlette and Wilcoxon, 1967
<i>Discoaster multiradiatus</i> Bramlette and Riedel, 1954
<i>Sphenolithus neoabies</i> Bukry and Bramlette, 1969
<i>Discoaster neohamatus</i> Bukry and Bramlette, 1969
<i>Chiasmolithus oamaruensis</i> (Deflandre, 1954) Hay, Mohler and Wade, 1966
<i>Gephyrocapsa oceanica</i> Kamptner, 1943
<i>Coccolithus pelagicus</i> (Wallich, 1877) Schiller, 1930
<i>Discoaster pentaradiatus</i> Tan 1927
<i>Sphenolithus predistentus</i> Bramlette and Wilcoxon, 1967
<i>Sphenolithus pseudoradians</i> Bramlette and Wilcoxon, 1967
<i>Reticulofenestra pseudoumbilica</i> (Gartner, 1967) Gartner, 1969
<i>Discoaster quinqueramus</i> Gartner, 1969
<i>Sphenolithus radians</i> Deflandre, 1952
<i>Helicosphaera recta</i> (Haq, 1966) Jafar and Martini, 1975
<i>Isthmolithus recurvus</i> Deflandre, 1954
<i>Helicosphaera reticulata</i> Bramlette and Wilcoxon, 1967
<i>Ceratolithus rugosus</i> Bukry and Bramlette, 1968
<i>Triquetrorhabdulus rugosus</i> Bramlette and Wilcoxon, 1967
<i>Discoaster saipanensis</i> Bramlette and Riedel, 1954
<i>Reticulofenestra samodurovii</i> (Hay, Mohler and Wade, 1966) Roth, 1970
<i>Helicosphaera sellii</i> (Bukry and Bramlette, 1969) Jafar and Martini, 1975
<i>Bramletteius serraculoides</i> Gartner, 1969
<i>Orthorhabdus serratus</i> Bramlette and Wilcoxon, 1967
<i>Zygodiscus sigmoides</i> Bramlette and Sullivan, 1961
<i>Chiasmolithus solitus</i> (Bramlette and Sullivan, 1961) Locker, 1968
<i>Coccolithus subdistichus</i> (Roth and Hay, 1967) Bukry, 1971
<i>Discoaster sublodoensis</i> Bramlette and Sullivan, 1961
<i>Discoaster surculus</i> Martini and Bramlette, 1963
<i>Discoaster tamalis</i> Kamptner, 1967
<i>Discoaster tani</i> Bramlette and Riedel, 1954
<i>Cruciplacolithus tenuis</i> Hay and Mohler, 1967
<i>Discoaster trinidadiansis</i> Hay, 1967
<i>Reticulofenestra umbilica</i> (Levin, 1966) Martini and Ritzkowski, 1968
<i>Discoaster variabilis</i> Martini and Bramlette, 1963
<i>Thoracosphaera</i> sp.
<i>Toweius</i> sp.
Mesozoic
<i>Tetralithus aculeus</i> (Stradner, 1961) Gartner, 1968
<i>Lithraphidites alatus</i> Thierstein, 1972
<i>Parhabdolithus angustus</i> (Stradner, 1963) Stradner, Adamiker and Maresch, 1968
<i>Reinhardtites anthophorus</i> (Deflandre, 1959) Perch-Nielsen, 1968
<i>Parhabdolithus asper</i> (Stradner, 1963) Manivit, 1971
<i>Watznaueria barnesae</i> (Black, 1959) Perch-Nielsen, 1968
<i>Lithraphidites carniolensis</i> Deflandre, 1963
<i>Lucianorhabdus cayeuxii</i> Deflandre, 1959
<i>Crucellipsis chiasia</i> (Worsley, 1971) Thierstein, 1972
<i>Markalius circumradiatus</i> (Stover, 1966)
<i>Vagalapilla compacta</i> Bukry, 1969
<i>Cretarhabdus conicus</i> Bramlette and Martini, 1964
<i>Biscutum constans</i> (Gorka, 1957) Black, 1967
<i>Cretarhabdus crenulatus</i> Bramlette and Martini, 1964
<i>Prediscosphaera cretacea</i> (Arkhangelsky, 1912) Gartner, 1968

Table 1. (Continued).

Mesozoic (Cont.)
<i>Arkhangelskiella cymbiformis</i> Vekshina, 1959
<i>Microrhabdulus decoratus</i> Deflandre, 1959
<i>Zygodiscus diplogrammus</i> (Deflandre, 1954) Gartner, 1968
<i>Cribrosphaerella ehrenbergii</i> (Arkhangelsky, 1912) Deflandre, 1952
<i>Parhabdolithus embergeri</i> (Noel, 1958) Stradner, 1963
<i>Lithastrinus floralis</i> Stradner, 1962
<i>Tetralithus gothicus</i> Deflandre, 1959
<i>Lithraphidites helicoideus</i> (Deflandre, 1959) Deflandre, 1963
<i>Assipetra infracretacea</i> (Thierstein, 1973) Roth, 1973
<i>Rucinolithus irregularis</i> Thierstein, 1972
<i>Stephanolithion laffitei</i> Noel, 1957
<i>Chiastocyclus litterarius</i> (Gorka, 1957) Manivit, 1971
<i>Rucinolithus magnus</i> Bukry, 1975
<i>Cyclagelosphaera margerelii</i> Noel, 1965
<i>Watznaueria oblonga</i> Bukry, 1969
<i>Vagalapilla octoradiata</i> (Gorka, 1957) Bukry, 1969
<i>Tranolithus orionatus</i> (Reinhardt, 1966a) Reinhardt, 1966b
<i>Broinsonia parca</i> (Stradner, 1963) Bukry, 1969
<i>Manivitella pemmatoides</i> (Deflandre ex Manivit, 1965) Thierstein, 1971
<i>Parhabdolithus regularis</i> (Gorka, 1957) Bukry, 1969
<i>Discorhabdus rotatorius</i> (Bukry, 1969) Thierstein, 1973
<i>Corollithion signum</i> Stradner, 1963
<i>Prediscosphaera spinosa</i> (Bramlette and Martini, 1964) Gartner, 1968
<i>Zygodiscus spiralis</i> Bramlette and Martini, 1964
<i>Parhabdolithus splendens</i> (Deflandre, 1953) Noel, 1969
<i>Micula staurophora</i> (Gardet, 1955) Stradner, 1963
<i>Tegumentum stradneri</i> Thierstein, 1972
<i>Vagalapilla stradneri</i> (Rood, Hay and Barnard, 1972) Thierstein, 1973
<i>Cretarhabdus surirellus</i> (Deflandre, 1954) Reinhardt, 1970
<i>Tetralithus trifidus</i> (Stradner, 1961) Bukry, 1973
<i>Eiffellithus turiseiffelii</i> (Deflandre, 1954) Reinhardt, 1965
<i>Braarudosphaera</i> sp.
<i>Cylindralithus</i> sp.

The very fine, clayey sediment is irregularly compacted, with holes in places, and is poorly structured. Clay particles are concentrated in large amorphous zones or in lamellae of variable thickness and of irregular shape. Nannofossils are visible only occasionally on the surfaces and are often deeply buried in the clay matrix, making their determination difficult. A red zeolitic claystone clast from the core catcher contained a few transported benthic foraminifers, but no calcareous nannofossils and no carbonate.

Sample 462-55-4, 55-59 cm (Plate 2, Figs. 4-6)

Pale brown, zeolitic marlstone contains 44% carbonate; rare deep-water benthic foraminifers, considered indigenous (Sliter, this volume); rare radiolarians; fish debris; and volcanic rock fragments.

Moderately etched and overgrown calcareous nannofossils dominate the nannofacies, despite the comparatively low carbonate content. Nannofossils are surrounded by a matrix of undulating clay laminae.

Sample 462-55-2, 117-122 cm (Plate 1, Figs. 1-3)

Brownish-gray claystone with 21% carbonate, and common, poorly preserved, mainly small planktonic and benthic foraminifers. Most benthic foraminifers are considered allochthonous, originating in shallower areas (Sliter, this volume).

Moderately well-preserved nannofossils are embedded in finely flaked, apparently diagenetically formed clay particles. Numerous fragments of coccoliths are dispersed in the fine clay matrix. No coccopheres were detected.

Sample 462-55-2, 71-73 cm (Plate 2, Figs. 1-3)

Tan, zeolitic marlstone contains 26% carbonate, common recrystallized radiolarians, little fish debris,

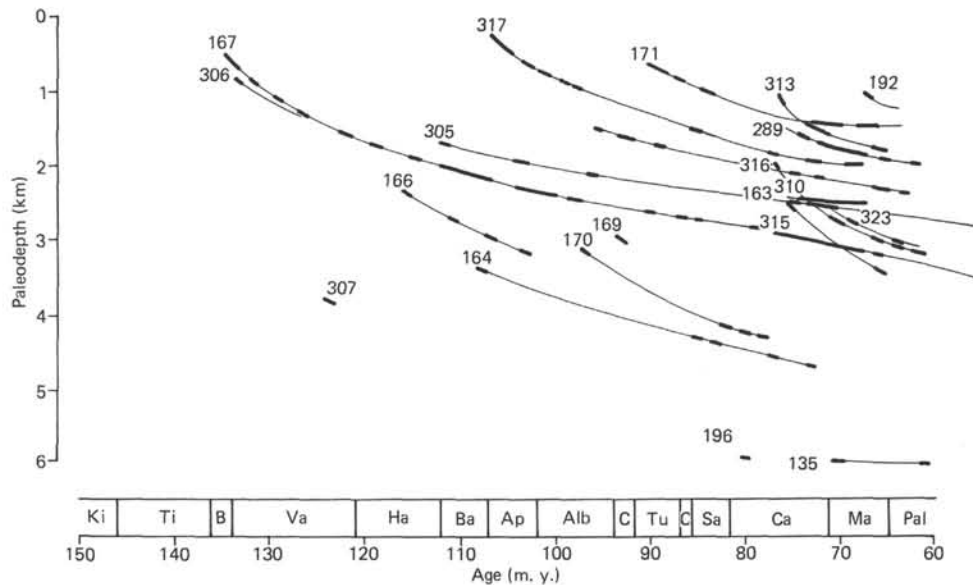


Figure 9. Back-tracked paleodepth of Pacific DSDP sites previously drilled on old oceanic crust (thin lines), and recovery of sediments (heavy lines). Modified from Thierstein (1979).

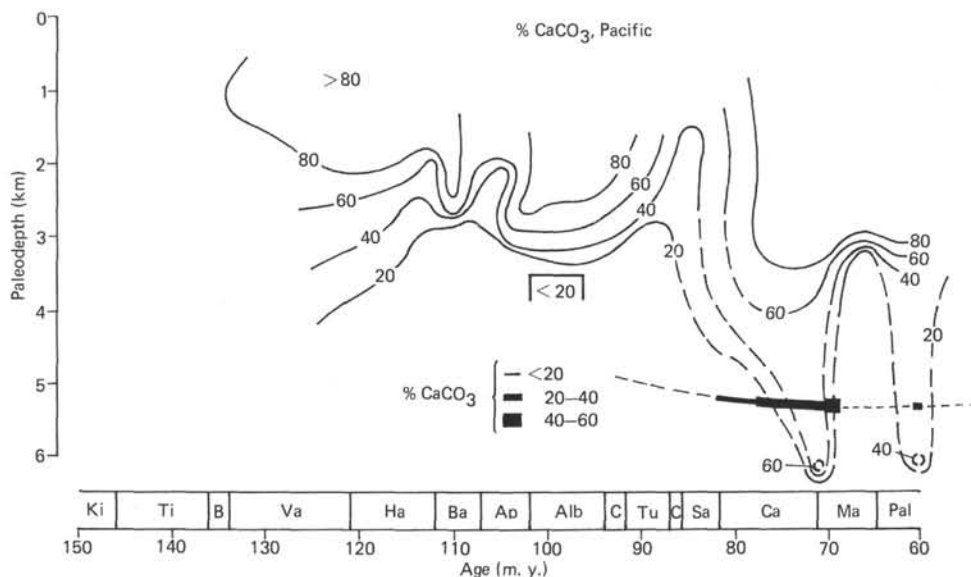


Figure 10. Mesozoic paleodepth and carbonate record of Site 462, and carbonate depositional patterns in the Pacific.

and few indigenous abyssal benthic foraminifers (Sliter, this volume).

Strongly etched and moderately overgrown nannofossils are dispersed in a compact clay matrix. Diagenetic dissolution of coccolith carbonate or diagenetic precipitation of clay minerals is evidenced by the occasional presence of coccolith imprints (e.g., Plate 2, Figs. 2, 3). No coccospheres were detected.

Sample 462-55-2, 64-66 cm (Plate 4, Figs. 1-6)

Dark brown, zeolitic clay contains 2% carbonate, rare silicified radiolarian casts, and few squashed benthic foraminifers.

Rare calcareous nannofossils observed in smear slides in occasional lithified clay clasts of over $50\ \mu\text{m}$ were not found by SEM. The matrix consists of non-structured clay particles and pockets of cristobalite spherules.

Sample 462-55-2, 61-64 cm (Plate 3, Figs. 1-3)

Tan marlstone, with 55% carbonate, contains few planktonic foraminifers and few transported as well as rare indigenous deep-water benthic foraminifers, rare fish debris, and common, recrystallized radiolarians.

Common, moderately well-preserved calcareous nannofossils are dispersed in coccolith debris and clay matrix. Occasional coccospheres are present.

Table 2. Samples with nannofacies analysis, Site 462.

Sample (interval in cm)	Sub-bottom Depth (m)	Age	Color of Sediment	Lithology	Abundance of Nannofossils	Provenance of Benthic Foraminifers (after Sliter, this volume)	CaCO ₃ (%)	Illustration
54-1, 39-45	509.39	Late Campanian	White	Chalk with laminations	Frequent	Transported	70	Pl 6, Figs. 4 to 6
54-1, 123-126	510.23	Late Campanian	White	Chalk with burrows	Common	Transported	69	Pl. 6, Figs. 1 to 3
54-2, 67-72	511.17	Late Campanian	White	Chalk	Common	Indigenous only	60	Pl. 5, Figs. 3, 5, 6
54-3, 3-7	512.03	Late Campanian	Grey	Chalk	Common	Transported	60	Pl. 5, Figs. 1, 2, 4
55-1, 85-89	514.35	Early Campanian	Brown	Marlstone	Common	Transported	50	Pl. 3, Figs. 4 to 6
55-2, 61-64	515.61	Early Campanian	Tan	Marlstone	Common	Transported	55	Pl. 3, Figs. 1 to 3
55-2, 64-66	515.64	Early Campanian	Brown	Claystone	Very rare	Indigenous only	2	Pl. 4, Figs. 1 to 6
55-2, 71-73	515.71	Early Campanian	Tan	Marlstone	Frequent	Indigenous only	26	Pl. 2, Figs. 1 to 3
55-2, 117-122	516.17	Early Campanian	Grey	Marlstone	Abundant	Transported	21	Pl. 1, Figs. 1 to 3
55-4, 55-59	518.55	Early Campanian	Brown	Marlstone	Abundant	Indigenous only	44	Pl. 2, Figs. 4 to 6
55,CC(A)	522.50	Early Campanian	Grey	Claystone	Rare	Indigenous only	16	Pl. 1, Figs. 4, 5, 6

Sample 462-55-1, 85-89 cm (Plate 3, Figs. 4-6)

Brown marlstone contains 50% carbonate and common planktonic and benthic foraminifers of dominantly small size, and benthic foraminifers, probably transported.

Common to abundant, moderately to well-preserved calcareous nannofossils are embedded in flaky clay matrix. No coccospheres were observed.

Sample 462-54-3, 3-7 cm (Plate 5, Figs. 1, 2, 4)

Gray, marly limestone contains 60% carbonate and few, poorly preserved planktonic and transported benthic foraminifers.

The nannofacies consists of abundant calcareous nannofossils embedded in a relatively coarse and porous matrix of mainly coccolith debris. Overgrowth features dominate over solution features. No coccospheres were observed.

Sample 462-54-2, 67-72 cm (Plate 5, Figs. 3, 5, 6)

White, marly limestone with burrows has carbonate content of 60% and contains only indigenous, deep-water benthic foraminifers. Strongly etched and moderately overgrown calcareous nannofossils are tightly packed with carbonate debris and clay particles, apparently in preferred orientation. Nannofacies very different from that of Sample 462-54-3, 3-7 cm, despite identical bulk carbonate content.

Sample 462-54-1, 123-126 cm (Plate 6, Figs. 1-3)

White marly limestone with darker laminations has a carbonate content of 69%. The coarse-fraction particles are all of relatively small size and include few planktonic and displaced (from up-slope) benthic foraminifers, rare radiolarians, and fish debris.

Common, moderately well-preserved and comparatively diverse calcareous nannofossils are found embedded in a matrix consisting mostly of nannofossil debris. Occasional coccospheres are present.

Sample 462-54-1, 39-45 cm (Plate 6, Figs. 4-6)

Brown, marly limestone with darker and lighter burrows has a carbonate content of 70%. Coarse fraction consists of abundant recrystallized radiolarians, and few poorly preserved planktonic and benthic foraminifers, probably displaced from up-slope.

Moderately to well-preserved, relatively diverse calcareous nannofossils are found embedded in porous matrix of nannofossil debris and clay. Degree of recrystallization is variable. Partially intact coccospheres are encountered very commonly.

It becomes evident from the descriptions and illustrations of the nannofacies that there are no systematic differences on a presence-absence basis between the nannofacies of samples with apparently transported benthic foraminifers and those with only indigenous abyssal benthics. In samples with transported benthic foraminifers, coccospheres are encountered more frequently and more consistently, and nannofossil diversity is higher than in samples with only indigenous deep benthics. Dissolution experiments with Late Cretaceous nannofossil assemblages (Thierstein, 1980) have shown that a few solution-resistant taxa tend to become enriched rapidly in poorly preserved assemblages by dissolution of most of the other members of the assemblage, leading to a decrease in diversity. Rapid burial of particles in transported horizons should tend to preserve the higher diversity of shallower-water fossil assemblages, and indeed higher diversities are observed in samples with transported benthics than in those with only indigenous benthic foraminifers (see last column in Figs. 7 and 8).

Campanian *Braarudosphaera* in the Nauru Basin

A unique morphotype of *Braarudosphaera* (sp. indet.) was found in the Campanian sediments of Cores 55 and 9A. All specimens are considerably overgrown, as illustrated in Plate 7. Overgrowth appears to occur preferentially along one of the cleavage planes of the individual trigonal calcite crystals of the pentolith, pos-

sibly aided by previous etching before burial. Asymmetric etching features on elements of pentoliths have been observed previously by Black (1972). The overgrowth of *Braarudosphaera* leads to buildup of the distal face and the development of a small central pit on the proximal side of the pentolith. The individual elements become radially asymmetric, and the sutures between the elements form an oblique, rather than perpendicular angle with the rotational-symmetry plane of the pentolith. *Braarudosphaera* (sp. indet.) are observed in samples with and without transported benthic foraminifers. The occurrence of *Braarudosphaera* in Holocene sediments is limited to well-preserved samples of less than 3 km water depth (Thierstein, 1980). Its apparent Recent pre-burial dissolution susceptibility and its occurrence in the Upper Cretaceous at Site 462 in samples with exclusively indigenous abyssal benthic foraminifers lend additional support to the interpretation of a descent of the CCD in the Pacific during the Campanian. The paleoecological and paleoceanographic implications of this first report of *Braarudosphaera* preserved in deep-sea sediments of Campanian age remain to be established.

ACKNOWLEDGMENTS

We thank Denise Noël for valuable discussions. Madame Cloiseau and the department of graphic arts (BRGM, Orléans) helped with the preparation of the manuscript and plates. Critical reviews by D. Bukry and F. Wind are acknowledged. Research was supported through NSF grant OCE76-22150 (H.R.T.) and through A.T.P. IPOD, R.C.P. 459 (H.M.).

REFERENCES

- Black, M., 1972. Crystal development in Discoasteraceae and Braarudosphaeraceae (planktonic algae). *Paleontology*, 15:476-489.
- Bukry, D., 1969. Upper Cretaceous coccoliths from Texas and Europe. *Univ. Kansas Paleontol. Contr.*, 5 (Protista 2).
- _____, 1973. Coccolith stratigraphy, eastern equatorial Pacific, Leg 16, Deep Sea Drilling Project. In van Andel, Tj. H., Heath, G. R., et al., *Init. Repts. DSDP*, 16: Washington (U.S. Govt. Printing Office), 653-711.
- _____, 1975. Coccolith and silicoflagellate stratigraphy northwestern Pacific Ocean, Deep Sea Drilling Project Leg 32. In Larson, R. L., Moberly, R., et al., *Init. Repts. DSDP*, 32, Washington (U.S. Govt. Printing Office), 677-701.
- _____, 1978. Biostratigraphy of Cenozoic marine sediments by calcareous nannofossils. *Micropaleontology*, 24:44-60.
- Martini, E., 1971. Standard Tertiary and Quaternary calcareous nannoplankton zonation. In Forniaci, A. (Ed.), *Proceedings of the II Planktonic Conference, Roma 1970* (Vol. 2): Rome (Ed. Technoscienza), 739-785.
- Noël, D., 1968. Nature et genèse des alternances de marnes et de calcaires du Barrémien supérieur d'Angles (Fosse vocontienne Basses-Alpes). *C. R. Acad. Sci. Paris*, 266:1223-1225.
- Noël, D., and Melguen, M., 1978. Nannofacies of Cape Basin and Walvis Ridge sediments, Lower Cretaceous to Pliocene (Leg 40). In Bolli, W. M., Ryan, W. B. F., et al., *Init. Repts. DSDP*, 40: Washington (U.S. Govt. Printing Office), 487-524.
- Roth, P. H., and Thierstein, H. R., 1972. Calcareous nannoplankton: Leg 14 of the Deep Sea Drilling Project. In Hayes, D. E., Pimm, A. C., et al., *Init. Repts. DSDP*, 14: Washington (U.S. Govt. Printing Office), 421-485.
- Thierstein, H. R., 1973. Lower Cretaceous calcareous nannoplankton biostratigraphy. *Abh. Geol. B.A. Wien*, 29.
- _____, 1979. Paleoceanographic implications of organic carbon and carbonate distribution in Mesozoic deep-sea sediments. In Talwani, M., and Ryan, W. B. F. (Eds.), *Deep Drilling Results in the Atlantic Ocean: Continental Margins and Paleoenvironment*: Washington (Am. Geophys. Union), pp. 249-274.
- _____, 1980. Selective dissolution of late Cretaceous and earliest Tertiary calcareous nannofossils: experimental evidence. *Cretaceous Res.*, 2:1-12.
- Verbeek, J. W., 1977. Calcareous nannoplankton biostratigraphy of middle and upper Cretaceous deposits in Tunisia, southern Spain and France. *Utrecht Micropaleont. Bull.*, 16.
- Winterer, E. L., 1973. Regional Problems. In Winterer, E. L., Ewing, J. I., et al., *Init. Repts. DSDP*, 17: Washington (U.S. Govt. Printing Office), 911-922.

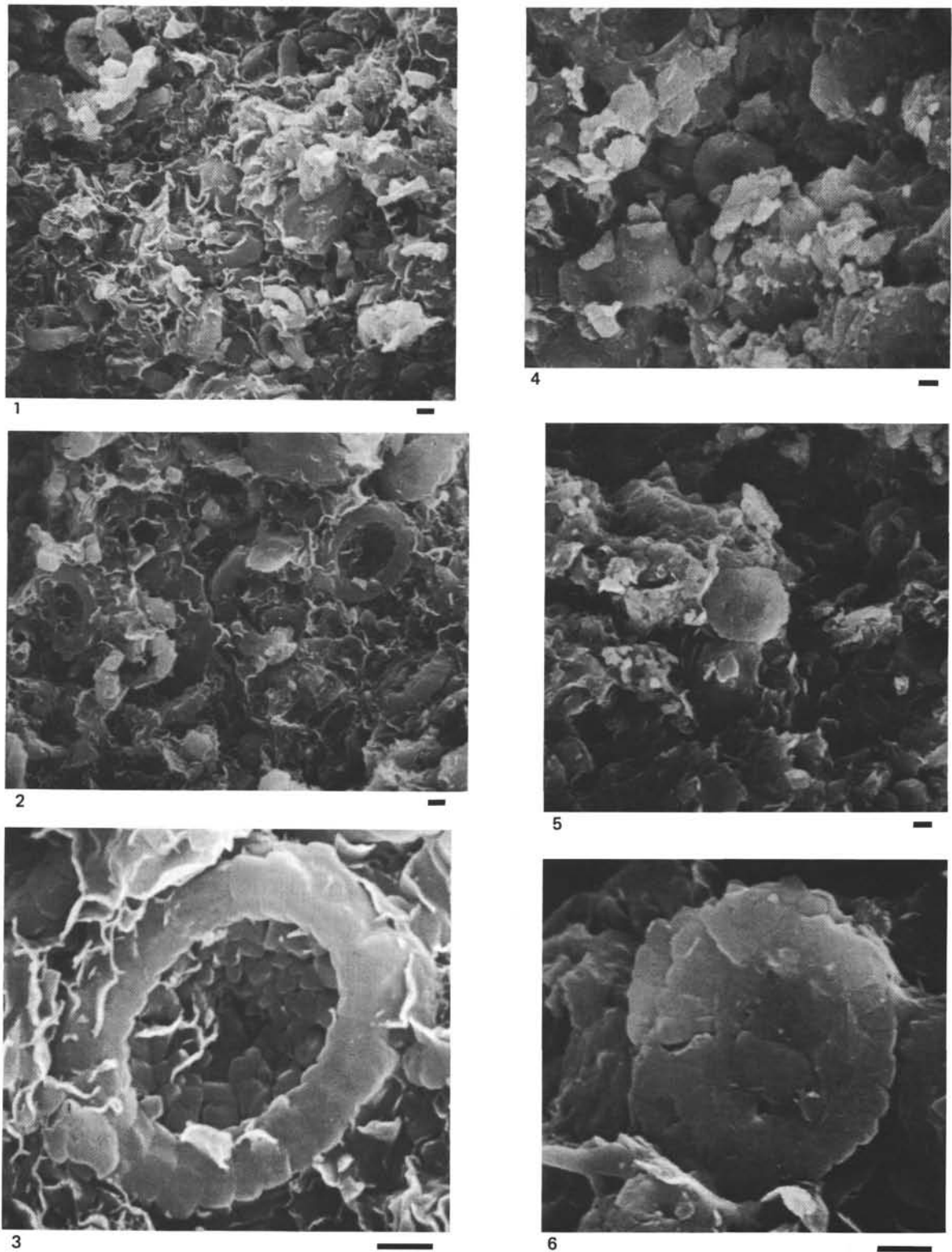
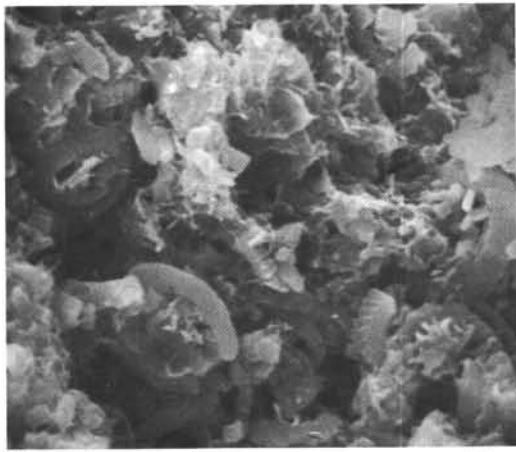


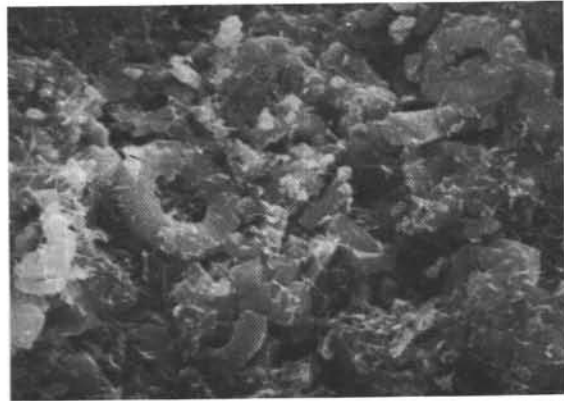
Plate 1. Scanning electron micrographs of lower Campanian nannofossils. Scale bars = 1 μ m.

Figures 1-3. Sample 462-55-2, 117-122 cm. Marly claystone with transported benthic foraminifers. 1, 2. Abundant, moderately etched and slightly overgrown nannofossils embedded in finely dispersed clay matrix, $\times 3000$. 3. Detail of 2, showing the proximal side of a slightly etched and overgrown coccolith, $\times 10,000$.

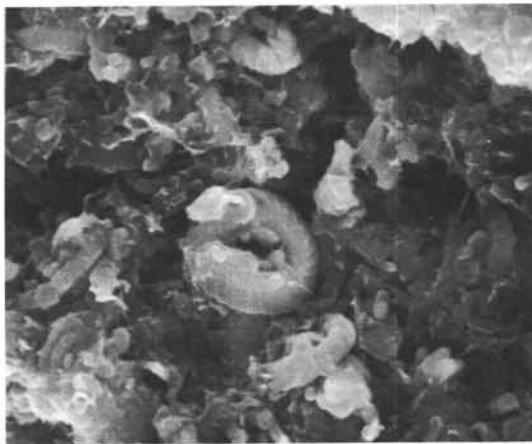
Figures 4-6. Sample 462-55, CC. Zeolitic marlstone with indigenous deep-water benthic foraminifers only. 4. *Watznaueria* spp. in a matrix of clay and overgrown carbonate particles, $\times 3000$. 5. *Cretarhabdus* spp. in a splintered, porous clay matrix, $\times 3000$. 6. Close-up of 5, showing etching and overgrowth of *Cretarhabdus* spp., whose central area structures are obscured by authigenic fused clay particles, $\times 10,000$.



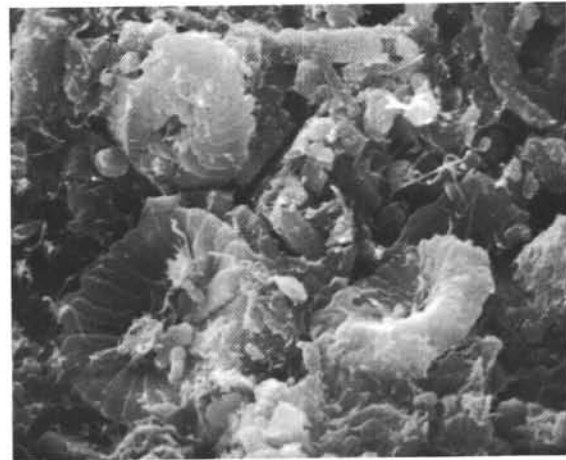
1



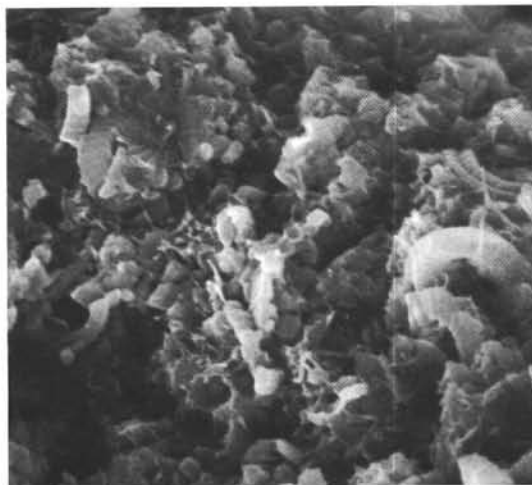
4



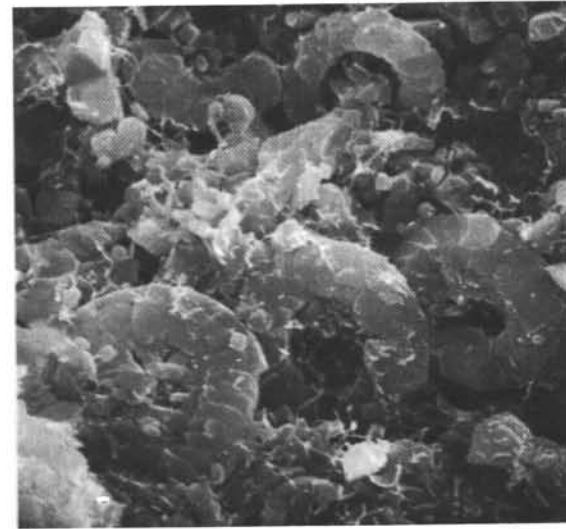
2



5



3



6

Plate 2. Scanning electron micrographs of lower Campanian nanofacies. Scale bars = 1 μ m.

Figures 1-3. Sample 462-55-2, 71-73 cm. Tan, zeolitic marlstone with indigenous deep-water benthic foraminifers only. 1. Common, strongly etched and broken nannofossils embedded in clay matrix, $\times 3000$. 2. Imprint of nannofossil in clay matrix, above strongly dissolved *Watznaueria barnesae*, (distal view) $\times 3000$. 3. Nannofossil remains dispersed in compact clay matrix with numerous imprints of coccoliths in upper half of photograph, $\times 3000$.

Figures 4-6. Sample 462-55-4, 55-59 cm. Zeolitic marlstone with indigenous deep-water benthic foraminifers only. 4. Moderately well-preserved calcareous nannofossils dominating the fine clay matrix. Fine threads are probably hyphae from post-recovery fungus growth, $\times 3000$. 5. Distal and proximal views of *Watznaueria barnesae* with signs of moderate overgrowth, $\times 5000$. 6. Placolith shields with central-area structures partially dissolved, embedded in fine-grained clay and coccolith-debris matrix, $\times 5000$.

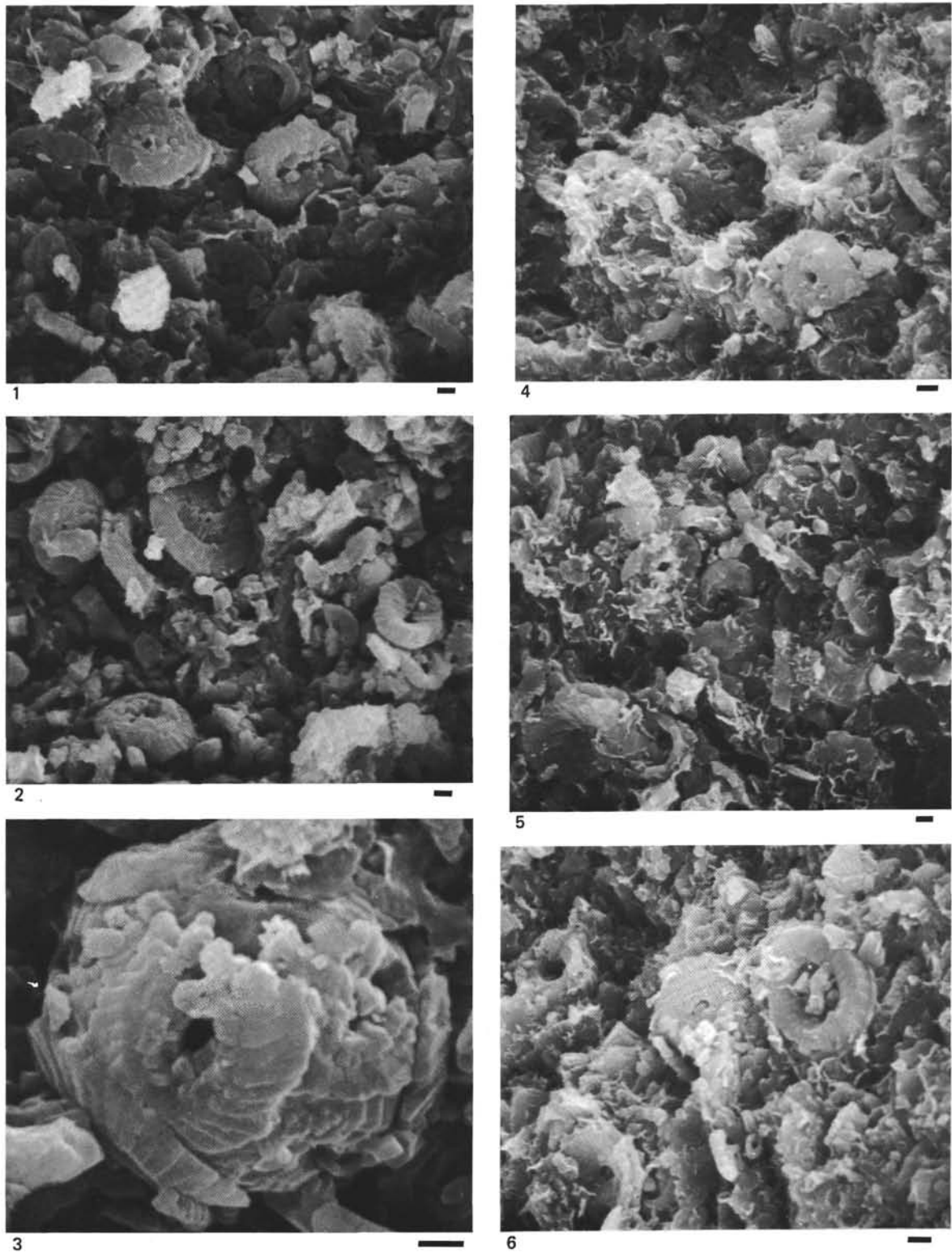
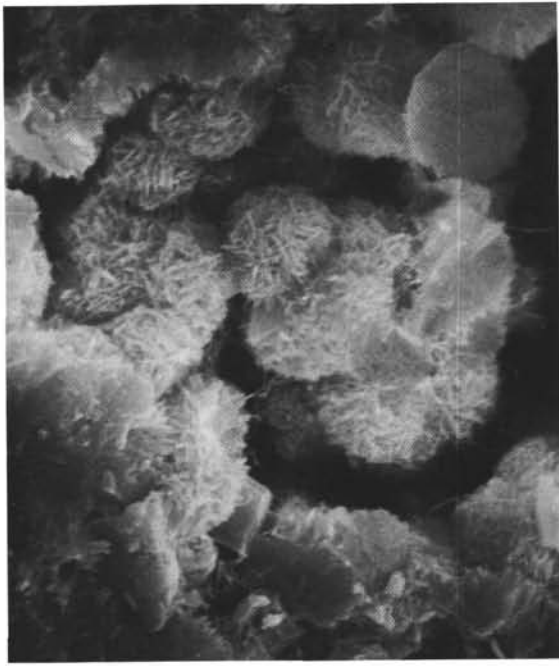


Plate 3. Scanning electron micrographs of lower Campanian nannofacies. Scale bars = 1 μ m.

Figures 1-3. Sample 462-55-2, 61-64 cm. Tan marlstone with transported benthic foraminifers. 1. Common calcareous nannofossils of dominantly solution-resistant taxa, dispersed in matrix of clay and coccolith debris, $\times 3000$. 2. Well-preserved *Cretarhabdus crenulatus* (distal view, upper center) and moderately well-preserved *Watznaueria barnesae* (distal views: upper left and lower left; proximal view: right center of micrograph), showing dissolu-

tion in central area and overgrowth of shield elements, $\times 3000$. 3. Coccosphere of *Watznaueria barnesae* with partially dissolved coccoliths, $\times 8000$.

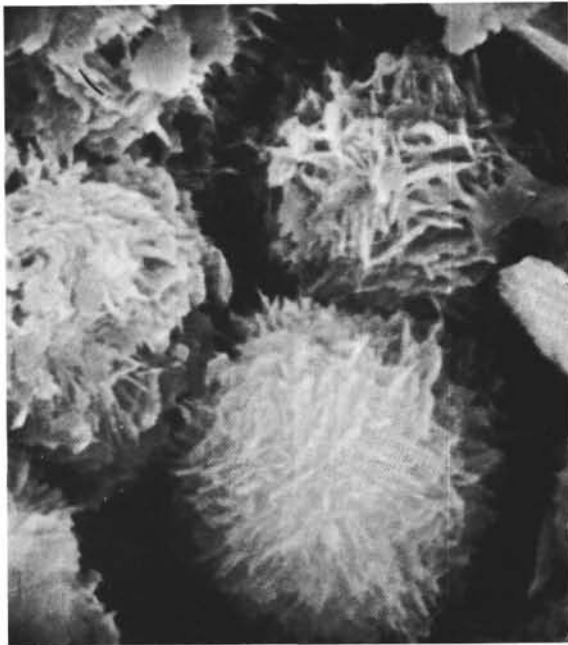
Figures 4-6. Sample 462-55-1, 85-89 cm. Brown marlstone with transported benthic foraminifers. 4. Moderately well-preserved calcareous nannofossils packed in dense clay matrix, $\times 3000$. 5, 6. Common, well-preserved, slightly overgrown calcareous nannofossils wrapped in flaky clay matrix, interspersed with coccolith debris, $\times 3000$ (5), $\times 4000$ (6).



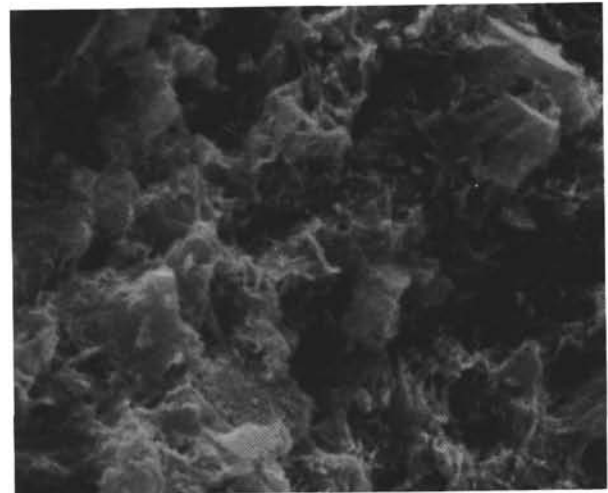
1



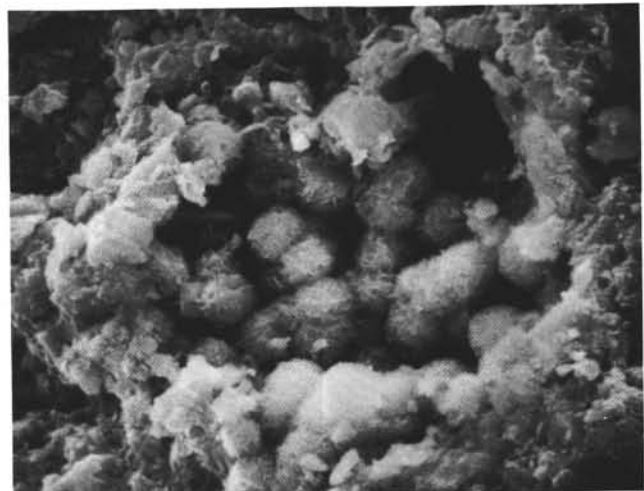
3



2



4

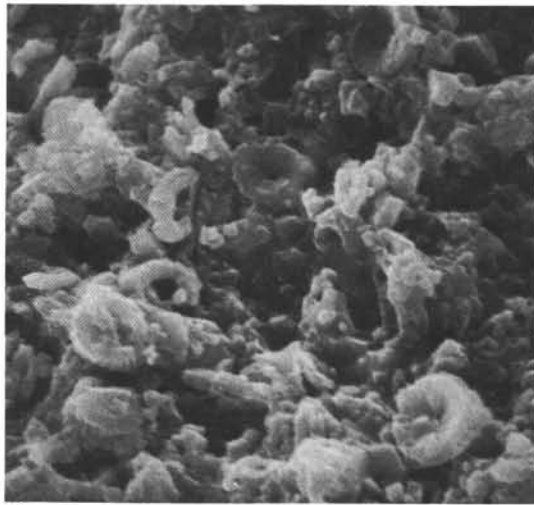


5

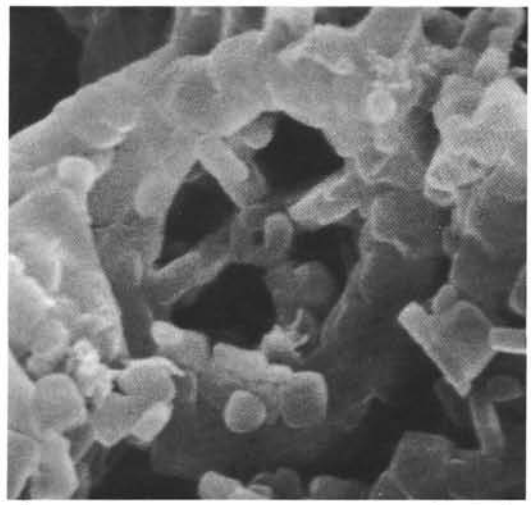
Plate 4. Scanning electron micrographs of lower Campanian nannofacies. Scale bars = 1 μ m.

Figures 1-5. Sample 462-55-2, 64-66 cm. Dark-brown claystone with indigenous benthic foraminifers only. 1, 2, 5. Aggregates of cristo-

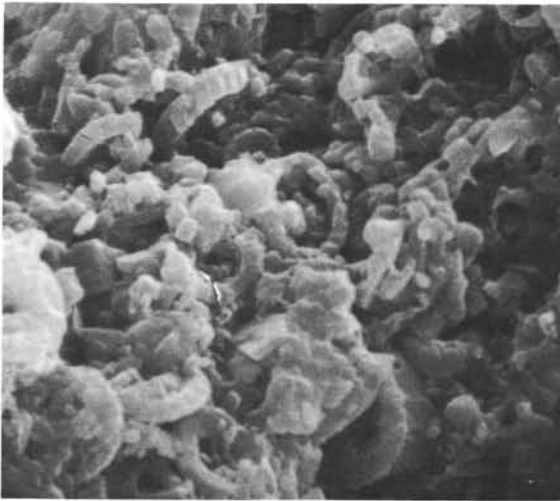
balite spherules developed diagenetically in fine clay matrix, $\times 2000$ (1), $\times 6000$ (2), $\times 1000$ (5). 3, 4. Poorly structured clay matrix, $\times 1000$ (3), $\times 2000$ (4).



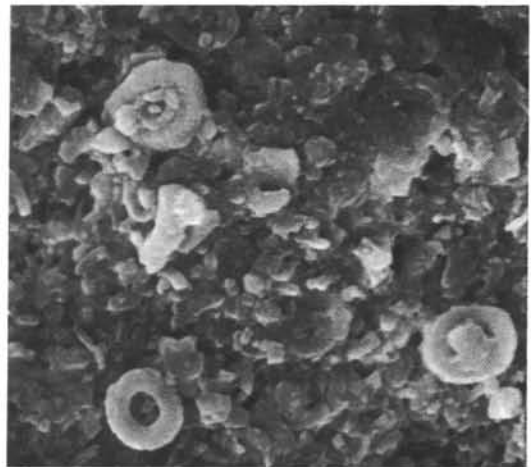
1



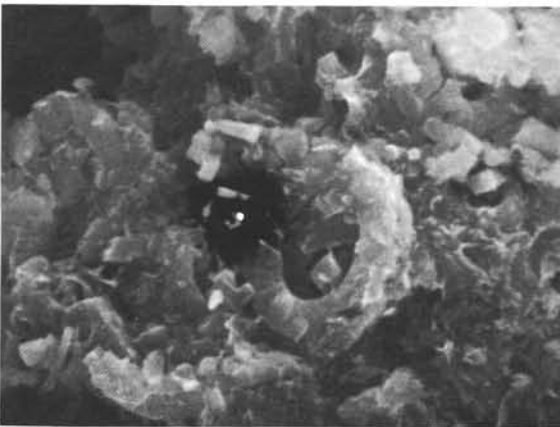
4



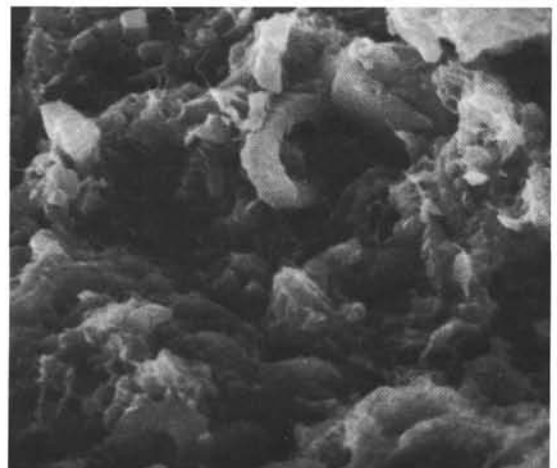
2



5



3

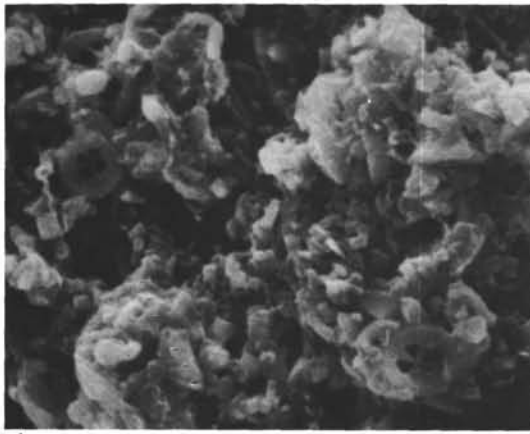


6

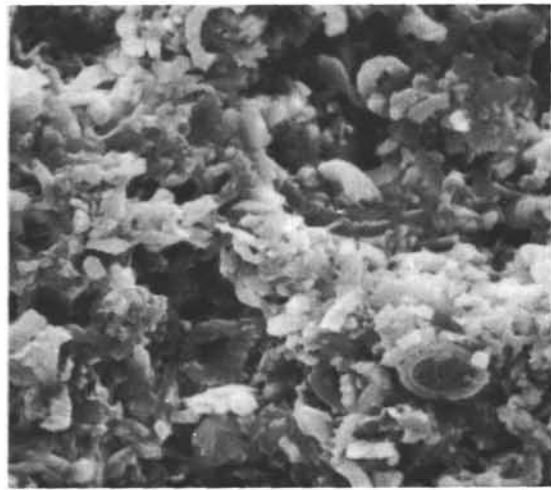
Plate 5. Scanning electron micrographs of upper Campanian nanofacies. Scale bars = 1 μm .

Figures 1, 2, 4. Sample 462-54-3, 3-7 cm. Marly limestone with transported benthic foraminifers. 1. Common, moderately overgrown calcareous nannofossils (mostly *Watznaueria barnesae*), embedded in rather porous coccolith debris and clay matrix, $\times 2000$. 2. Moderately etched and overgrown nannofossils in porous matrix

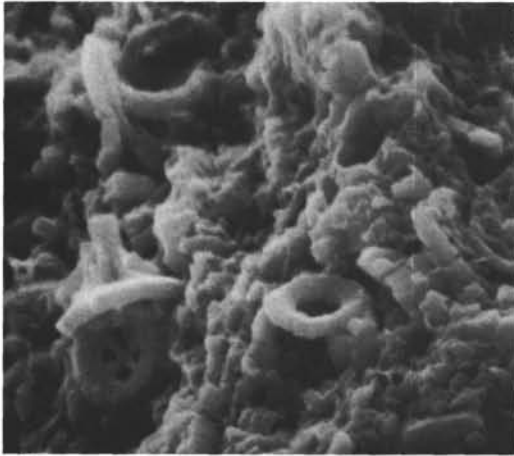
consisting dominantly of relatively coarse carbonate debris, $\times 3000$. 4. Proximal view of *Prediscosphaera cretacea*, showing fusion of elements with carbonate debris by overgrowth, $\times 10,000$. Figures 3, 5, 6. Sample 462-54-2, 67-72 cm. Marly limestone with indigenous benthic foraminifers only. 3, 6. Few, strongly etched nannofossil shields are packed in dense matrix of clay particles and coccolith debris, $\times 3000$. 5. Coccoliths and clay particles, showing preferred orientation, $\times 2000$.



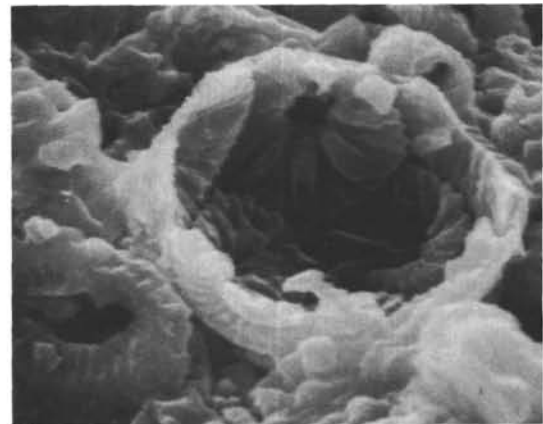
1



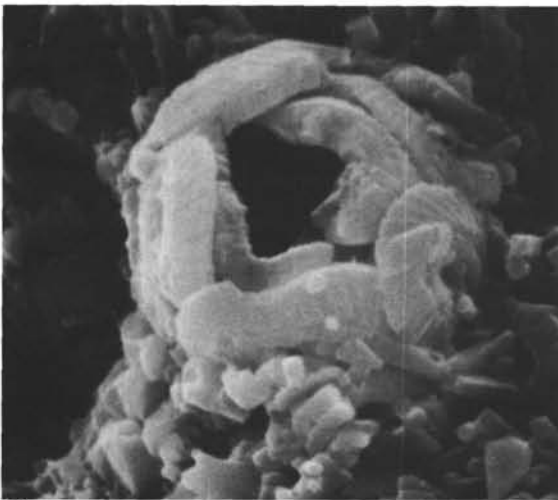
4



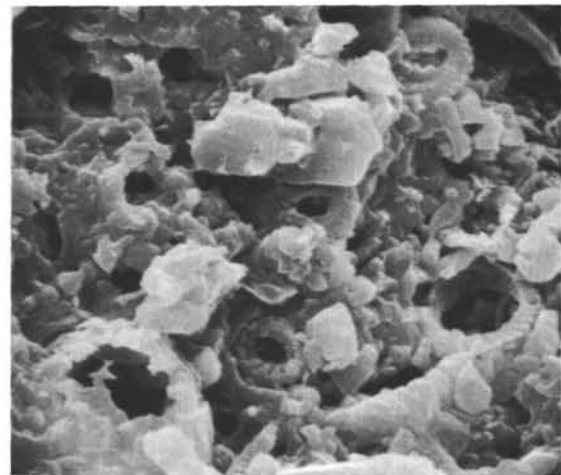
2



5



3



6

Plate 6. Scanning electron micrographs of upper Campanian nannofacies. Scale bars = 1 μm .

Figures 1-3. Sample 462-54-1, 123-125 cm. Laminated, marly limestone with transported benthic foraminifers. 1, 2. Nannofossils and nannofossil debris, making up the bulk of the sediment, solution-susceptible *Prediscosphaera cretacea* abundant, $\times 2000$ (1), $\times 3000$ (2). 3. Coccosphere of *Watznaueria barnesae*, partially dissolved, $\times 5000$.

Figures 4-6. Sample 462-54-1, 39-45 cm. Burrowed marly limestone with transported benthic foraminifers. 4. Nannofossils and nannofossil debris dispersed in relatively coarse-grained clay matrix, $\times 2000$. 5. Broken coccosphere of *Cyclagelosphaera margerellii*, showing overgrowth on proximal shields, *Watznaueria barnesae* in left lower corner strongly dissolved, $\times 6000$. 6. Moderately well-preserved nannofossils dispersed in relatively coarse and porous carbonate debris and clay matrix, coccosphere of *Watznaueria barnesae* in lower left corner, $\times 2000$.

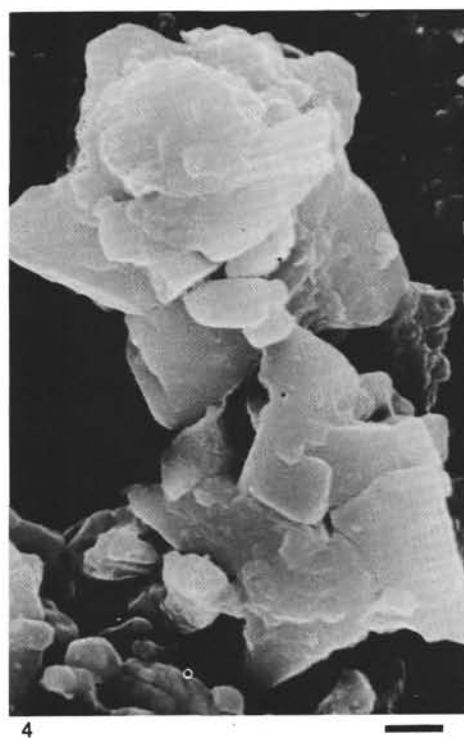
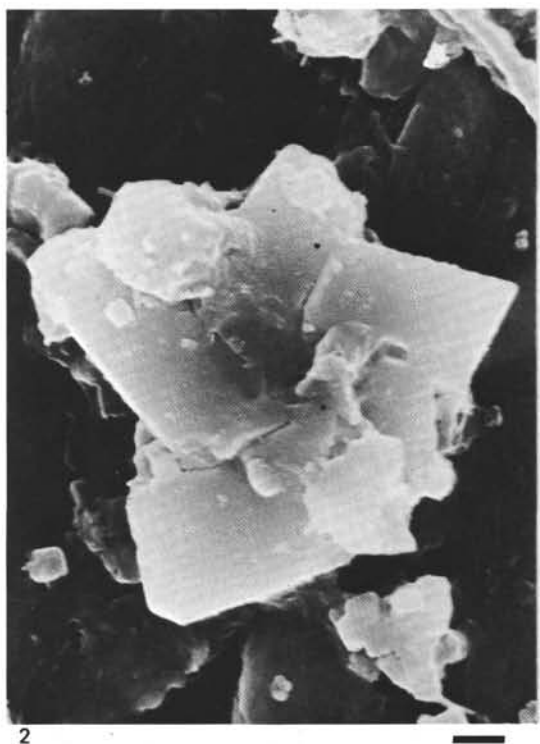
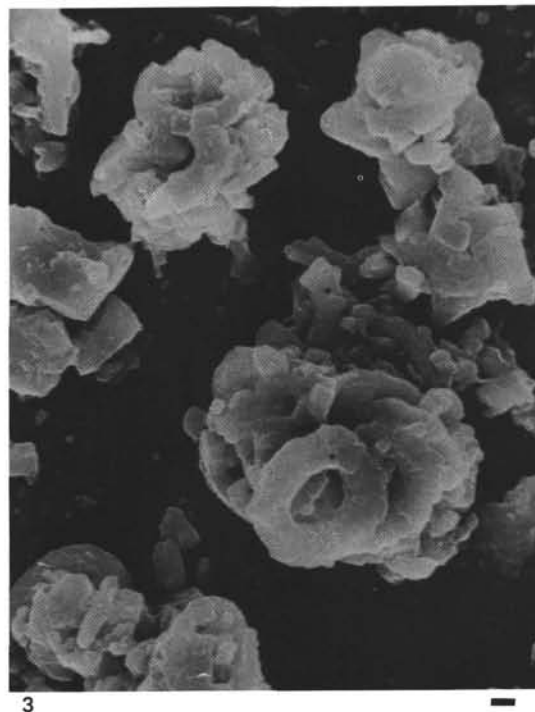
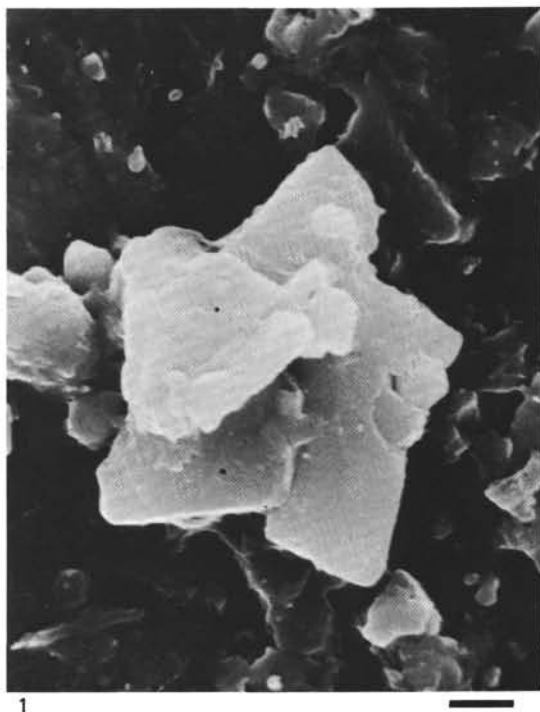


Plate 7. Scanning electron micrographs of early Campanian *Braarudosphaera* (sp. indet.) in disaggregated Sample 462-55-4, 37-40 cm. Scale bars = 1 μ m.

Figure 1. Proximal view of pentalith, showing overgrowth of calcite crystals, incorporating carbonate debris and leading to radial asymmetry of pentalith, $\times 9800$.

Figure 2. Proximal view of asymmetric pentalith showing central pit, $\times 7400$.

Figure 3. Moderately well-preserved nannofossils with two specimens of *Braarudosphaera* (sp. indet.), $\times 3200$.

Figure 4. Distal view of *Braarudosphaera* (sp. indet.) in upper part of micrograph, showing sloping, re-calcified crystal surfaces; central part obscured by debris; proximal view of *Braarudosphaera* (sp. indet.) in lower part of micrograph, with interlocking overgrowth features on some elements, $\times 8600$.